© IWA Publishing 2016
373

Water Practice & Technology Vol 11 No 2
doi: 10.2166/wpt.2016.044

Application of a rainfall-runoff model for regional-scale flood inundation mapping for the Langat River Basin

Majid Mirzaei[a,*], Mina Faghih[b], Tan Pei Ying[b], Ahmed El-Shafie[b], Yuk Feng Huang[a] and Juneseok Lee[c]

[a] Lee Kong Chian Faculty of Engineering and Science, Universiti Tunku Abdul Rahman, Kuala Lumpur, Malaysia

[b] Civil Engineering Department, Faculty of Engineering, University of Malaya, 50603 Kuala Lumpur, Malaysia

[c] Department of Civil and Environmental Engineering, San Jose State University, San Jose, CA, USA

* Corresponding author. E-mail: mirzaeii@gmail.com

Abstract

Rapid growth in recent decades has changed engineering concepts about the approach to controlling storm water in cities. Over the past years flood events have occurred more frequently in several countries in the tropics. In this study the behavior of Langat River in Malaysia was analyzed using the hydrodynamic modeling software (HEC-RAS) developed by the 'Hydrologic Engineering Center, U.S. Army Corps of Engineers', to simulate different water levels and flow rates corresponding to different return periods from the available database. The aim was to forecast peak flows, based on rainfall data and the maximum rate of precipitation in different return periods in storms of different duration. The maximum flows were obtained from the Automated Geospatial Watershed Assessment tool for the different return periods, and the peak flows from extreme rainfall were applied to HEC-RAS to simulate different water levels and flow rates corresponding to different return periods. The water level along the river and its tributaries could then be analyzed for different flow conditions.

Key words: flood, flood mapping, HEC-RAS, KINEROS2

INTRODUCTION

Floods are among the most destructive events that occur, causing huge losses in terms of life and economics. Many studies have been carried out to forecast flood probability and predict losses. Flood forecasting is mainly influenced by hydrologic data, the availability of which are subject to various unpredictable factors including antecedent conditions and precipitation. Significant improvements are needed in the systems used to predict the floods. With the increasing magnitude and frequency of extreme hydrological events–e.g., droughts and floods–it is important to develop models capable of estimating floods reasonably accurately using the data available. When urban development spreads onto flood plains, this reduces floodwater storage and diversion routes. The impact of urbanization includes alteration of a watershed's response to rainfall, increasing volumes and peak flows, and flood risk downstream, reducing low flows and increasing pollution (Brilly Rusjan & Vidmar 2006).

Prata *et al.* (2011) focused on the application of HEC-RAS to analyzing river behavior and studied the Taquaracu River in the City of Ibiracu, in Brazil using maximum flows derived from rainfall data. HEC-RAS was used with these to compute water levels along the river and its tributaries under different flow conditions. Merwade *et al.* (2008) proposed the use of GIS techniques for creating river terrain models. These were first applied and then cross-validated using data for three study reaches: the Brazos River in Texas, the Kootenai River in Montana, and Stroud's Creek in North Carolina.

Downloaded from https://iwaponline.com/wpt/article-pdf/11/2/373/381751/wpt0110373.pdf
by guest

Water Practice & Technology Vol 11 No 2
doi: 10.2166/wpt.2016.044

Solaimani (2009) integrated GIS and HEC-RAS to use hydraulic analysis to separate the high- and low- risk areas on the floodplain. The results from HEC-RAS were displayed using GIS.

To predict floods, accurate runoff data are required. One computer model that has become increasingly popular is the Kinematic Runoff and Erosion Model, KINEROS2 (K2). In addition to K2, the Automated Geospatial Watershed Assessment (AGWA) tool is a versatile means of hydrologic analysis that: (1) provides a simple, direct and repeatable method for hydrologic modeling; (2) makes it possible to use GIS databases; (3) is compatible with other geospatial basin analysis software environments (Mirzaei *et al.* 2014); and (4) is useful for developing alternative scenarios and future simulation works at multiple scales (Miller *et al.* 2002; Goodarzi *et al.* 2012; Mirzaei *et al.* 2013). AGWA provides the functionality for modeling and evaluation using the Soil and Water Assessment Tool and K2. Nedkov & Burkhard (2011) reiterated the modeling process in the AGWA GIS environment with five main steps–watershed delineation and discretization, vegetation cover and soil parameters, precipitation writing files, running the model, and visualizing the results.

The main objective of this study was to develop a model to delineate the flood plain. The idea behind it was to use a model to analyze the Langat River Basin's behavior under different conditions using advanced technologies. Within this objective, the aims of the study were to: analyze the frequency analysis maximum rate of rainfall annually for different durations, simulate different water levels and flow velocities corresponding to different return periods from the available database using HEC-GeoRAS and HEC-RAS, and analyze the water level along the Langat River and its tributaries, under different flow conditions.

METHODOLOGY

Study area

The Langat River is in the south of the densely populated Klang River Basin, in Malaysia. It is approximately 78 km long and drains about 2,350 km^2 (Zakaria 2008). Its headwaters are in the Gunung Nuang and it flows via urban centers like Hulu Langat, Seremban to the Straits of Malacca (Figure 1)

Frequency analysis of maximum annual rainfall

Probability density function of annual maximum discharge

The annual maximum rainfall is among the important parameters in hydrologic studies that can be used for flood design. To estimate the least probable rainfall maxima, which have high return periods, the extreme data were fitted to theoretical probability distributions. This indicated that the generalized extreme value (GEV) distribution was the best fit for the annual maxima for all sites in the study area. The GEV distribution is a flexible, three-parameter model that combines the Gumbel, Frechet, and Weibull maximum extreme value distributions. Throughout this study, a GEV distribution was used to fit the annual rainfall maxima at the gauging stations for year t (t = 1, …, T). The probability density function, f, and the cumulative density function, F, of a GEV (μ, λ, ξ), where μ, λ and ξ are the location, scale and shape parameters, respectively, are given by:

$$f(x|\mu,\ \lambda,\ \xi) = (1/\lambda)\ [1 - \xi(x-\mu)/\lambda]^{\frac{1}{\xi} - 1} \times \exp\{-[1 - \xi(x-\mu)/\lambda]^{\frac{1}{\xi}} \tag{1}$$

$$F(x|\mu, \lambda, \xi) = \exp\left\{-[1 - \xi(x-\mu)/\lambda]^{1/\xi}\right\} \tag{2}$$

Downloaded from https://iwaponline.com/wpt/article-pdf/11/2/373/381751/wpt0110373.pdf
by guest

Water Practice & Technology Vol 11 No 2
doi: 10.2166/wpt.2016.044

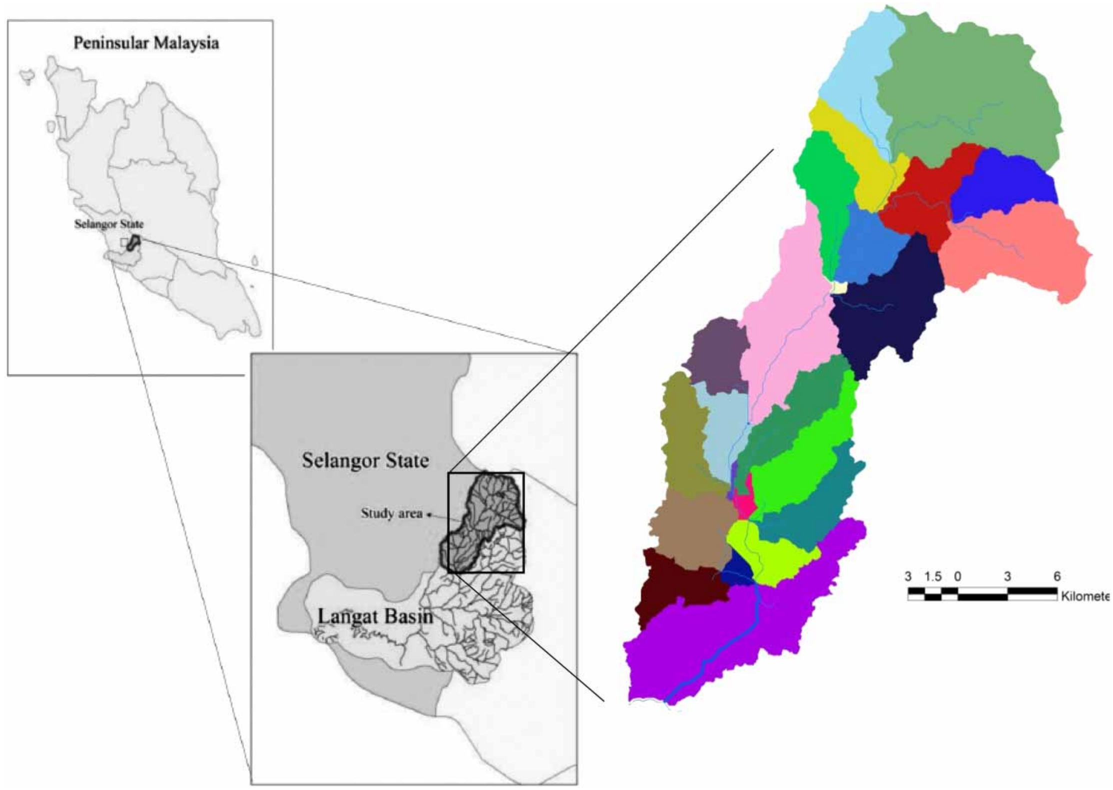

Figure 1 | Location of the Langat River Basin.

$\lambda > 0; \xi \neq 0; 1 - \xi(x - \mu)/\lambda > 0$

The case $\xi = 0$ corresponds to the Gumbel distribution, and is equal to the limit of Equation (1) when $\xi \rightarrow 0$

$$f(x|\mu, \lambda) = (1/\lambda) \exp\left\{-\frac{(x-\mu)}{\lambda} - \exp\left(-\frac{(x-\mu)}{\lambda}\right)\right\} \tag{3}$$

$$F(x|\mu, \lambda) = \exp\left\{-\exp\left(-\frac{(x-\mu)}{\lambda}\right)\right\} \tag{4}$$

$\lambda > 0$

The main purpose of frequency analysis is to estimate the parameter vector $\theta = (\mu, \ \lambda, \xi)$.

Flood mapping

HEC-RAS represents floodplains as computed water surface elevations at every cross-section (Figure 2). During data import, these and the distance from the stream centerline to the left and right floodplain boundaries, are brought into ArcGIS and stored in the cross-section parameter table. Hence, two things are known about the floodplain at each cross-section: the water surface elevation and lateral extent of the plain. The water surface profiles are mapped on the basis of the cross-section lines. The script requires the cross-section line theme and parameter table as inputs. The output is also a line theme, identical to the cross-section theme in location and orientation, but not as wide. The cross-sections in the HEC-RAS model should be wide enough to contain the computed water surface elevations. Using the water surface profile at each cross-section, a triangulated irregular network

Downloaded from https://iwaponline.com/wpt/article-pdf/11/2/373/381751/wpt0110373.pdf
by guest

doi: 10.2166/wpt.2016.044

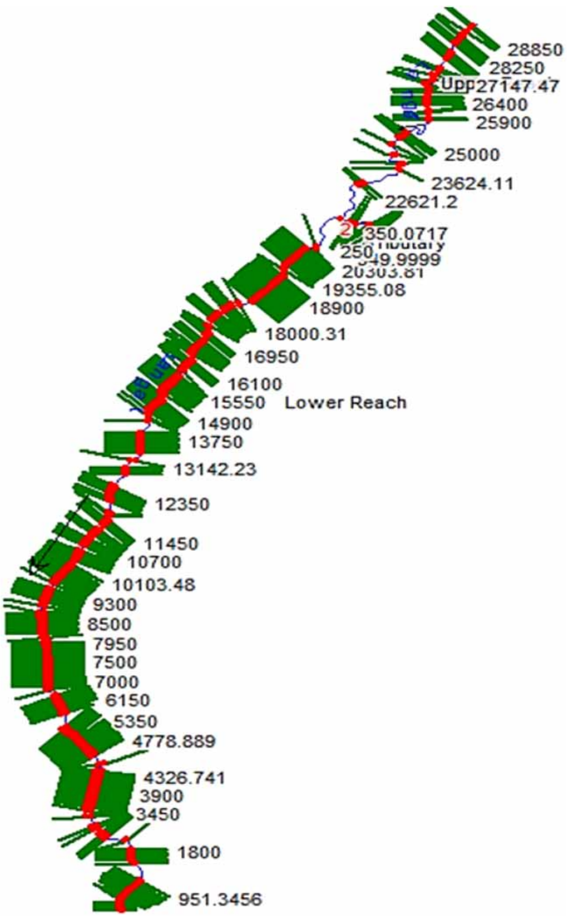

Figure 2 | Cross-Sections along the Langat River.

(TIN) representing the entire floodwater surface can be constructed using the Surface/Create TIN from the 'Features' menu option in ArcGIS. The water surface lines are used as break-lines, and the cross-section bounding polygon is used to define the areal extent of the water surface. When viewed together with the terrain TIN, flooded areas can be seen.

HEC-GeoRAS (GIS) preprocessing

The geometry set-up in HEC-GeoRAS involves digitizing the stream centerline, predicting overbank flowlines, levees, and providing polygon coverage delineating surface roughness. This was facilitated by visual interpretation of the Digital Terrain Model, and comparison of channel and floodplain cover, with estimates of the channel's roughness characteristics using Hicks & Mason (1998) method and the floodplain. Finally, very closely spaced cross-sections were digitized, ensuring that these were kept as perpendicular to the line of flow as possible. Because the primary channel meanders across the active gravel channel, changing direction frequently, the placement of section lines takes considerable effort as HEC-RAS requires that cross-sections do not overlap anywhere. Channel and cross-section lines are then encoded with z values from a TIN surface. Finally, pre-processed geometry data were exported to HEC-RAS. (Howard *et al.* 2012)

Modeling in HEC-RAS

HEC-RAS was developed for one-dimensional and unsteady flow hydraulic calculations, and sediment transport modeling (Brunner 2006). Under steady flow conditions, HEC-RAS calculates

Downloaded from https://iwaponline.com/wpt/article-pdf/11/2/373/381751/wpt0110373.pdf
by guest

Water Practice & Technology Vol 11 No 2
doi: 10.2166/wpt.2016.044

water surface profiles based on the input geometry, the gradient, and Manning's n for any number of discharge rates. Water surface profiles referenced in the software are equivalent to trim-lines, wash limits, or peak-flow water heights. The system is capable of modeling channel networks or a single reach, and provides modeling of subcritical, supercritical, and mixed–i.e., a mixture of subcritical, critical, and supercritical flow–flow regimes (Brunner 2006). HEC-RAS calculates water surface profiles for successive channel cross-sections by solving the energy equation using the standard step-backwater method. Conveyance, channel velocity, and energy loss are accounted for by Manning's equation. To use HEC-RAS effectively for steady flow in natural channels several assumptions are made: (1) flow is steady, (2) flow varies gradually along the reach, (3) flow is one-dimensional, and (4) the channel slope is low ($<10\%$) (Brunner 2001; Howard *et al.* 2012).

HEC-GeoRAS (GIS) post-processing

The predicted extent of inundation was derived by exporting the HEC-RAS output water surface to HEC-GeoRAS, where the water surface was overlaid, showing excellent correspondence with the flood inundation delineated. Once in GeoRAS, inundation data for each modeled scenario were converted to TINs and then GRID surfaces. Velocity data were exported to GeoRAS in point format, each point representing the estimated velocity at a cross-section. These were also interpolated to a TIN, and the vertices converted to a GRID form and overlaid onto their respective terrain surfaces for validity checking. HEC-RAS includes tools that can be used to simulate raising or lowering the bed level, and to simulate damming. These were explored and evaluated, to determine whether they were more or less effective than the terrain modeling approach when using high resolution (z) geometry (Howard *et al.* 2012).

KINEROS2

The KINEROS rainfall-runoff-erosion model was developed in the 1970s and has continued to evolve and improve (Woolhiser *et al.* 1990; Goodrich *et al.* 2006). It is now known as KINEROS2 (K2). It is a physical-event based, distributed and dynamic model that predicts surface runoff, erosion losses, infiltration amount and interception depth from the watershed, arising predominantly from overland flow. The watershed is approximated by a cascade of overland flow planes, channels and impoundments. The flow planes can be split into multiple components with different slopes, roughness, soils, etc., and contiguous planes can have different widths. In an overland flow conceptual model, small-scale spatial distribution of infiltration variability can be represented and parameterized for numerical efficiency, and the micro-topography is inserted into the simulation. In most urban element models, the runoff is based on the pervious and impervious fractions. In K2, however, infiltration is dynamic, and interacts with both rainfall and runoff. The conceptual infiltration model incorporates two layers in the soil profile, and soil moisture is redistributed during any hiatus in the storm.

Overland flow is treated as one-dimensional, with flux estimated as:

$$Q = \alpha h^m \tag{5}$$

where: Q is discharge per unit width and h is the storage of water per unit area. Slope, roughness and flow regime are determinants of coefficients α and m.

Downloaded from https://iwaponline.com/wpt/article-pdf/11/2/373/381751/wpt0110373.pdf
by guest

Water Practice & Technology Vol 11 No 2
doi: 10.2166/wpt.2016.044

Model calibration and sensitivity analysis

The model is calibrated using mean areal rainfall as well as daily runoff records. The statistical criterion used in this study was Nash-Sutcliffe Efficiency (NSE), calculated as:

$$E = 1 - \frac{\sum_{t=1}^{N} \left(Q_o^t - Q_m^t \right)^2}{\sum_{t=1}^{N} \left(Q_o^t - \overline{Q_o} \right)^2} \tag{6}$$

where: Q_o^t = observed discharge at time t; Q_m^t = modelled discharge at time t; $\overline{Q_o}$ = mean of observed data; and, N = total number of observations. NSE ranges between $-\infty$ and 1.0 (1 inclusive), with NSE = 1 being the optimal value. Values between 0.0 and 1.0 are generally viewed as acceptable levels of performance, whereas values below 0.0 indicate that the mean observed value is a better predictor than the simulated value–i.e., performance is unacceptable. An efficiency of zero indicates that the model's predictions are as accurate as the mean of the observed data. Essentially, the closer the model's efficiency is to 1, the more accurate the model is Nash & Sutcliffe (1970) and Moriasi *et al.* (2007).

Sensitivity of the model to change was based on a selected set of parameters. By modifying them from their initial value, the degree of change in peak runoff was determined for each event, so that those sensitive to changes in peak runoff were identified. The parameters evaluated in this way were–saturated hydraulic conductivity (Ks_Ch and Ks_Ul), Manning's n (n_Ch and n_Ul), mean capillary drive (G_Ch and G_Ul), all for channels and uplands respectively, and coefficient of variation of Ks (CV_Ks), upland interception (I_Ul), and rain-splash coefficient (C_f).

RESULT AND DISCUSSION

The Langat River modeling resulted in the creation of flood extent and hazard, water depth and flow velocity maps. These were analyzed to derive explanations for various scenarios.

Rainfall depth-duration frequency curves

A GEV distribution was fitted separately to the running annual maxima for durations of 15, 30, 60, 90 and 120 minutes, for time-series data. Table 1 shows the estimated GEV parameters μ, γ and K. As expected μ increases with increasing duration.

By choosing a return period T, the rainfall depth x (mm) can be plotted as a function of duration D. Figure 3 shows the depth-duration frequency (DDF) curves for T = 5, 25, 50 and 100 years. There is a strong increase of rainfall depth with D, e.g. for T = 100 years rainfall depths range from 68 to 219 mm for values of D rising from 15 to 120 minutes (Figure 3).

Table 1 | Estimated GEV parameters for D = 15, 30, 60, 90 and 120 min

D (min)	*μ*	*γ*	*k*
15	28.676	0.097	0.2441
30	47.129	0.223	0.1562
60	67.099	0.228	0.1896
90	75.676	0.228	0.1519
120	78.088	0.255	0.1743

Downloaded from https://iwaponline.com/wpt/article-pdf/11/2/373/381751/wpt0110373.pdf
by guest

Water Practice & Technology Vol 11 No 2
doi: 10.2166/wpt.2016.044

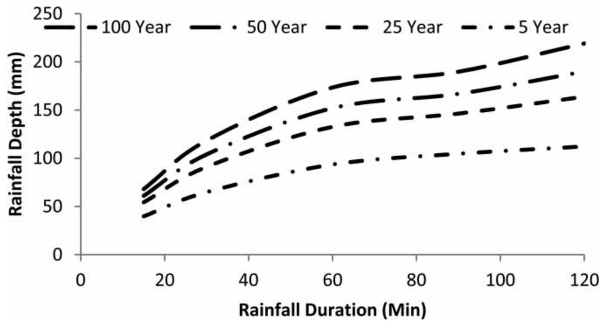

Figure 3 | Rainfall DDF curves for return periods of 5, 25, 50 and 100 years.

Rainfall-runoff modeling

The discharge data were obtained from K2, which simulates the hydrologic elements of a meteorological event like peak flow and infiltration (Nikolova *et al.* 2009; Mirzaei *et al.* 2013). As runoff data are available for the basin outlet, the model was calibrated and validated on the basis of three events there. The NSE calculated for the calibrated model was 0.88 and the model was validated using data from storm events in the same year as those used for calibration. The NSE for this event was 0.74, which is reasonably good.

The results show that the theoretical result from K2 is close to the observed data, so the results are acceptable (Figure 4).

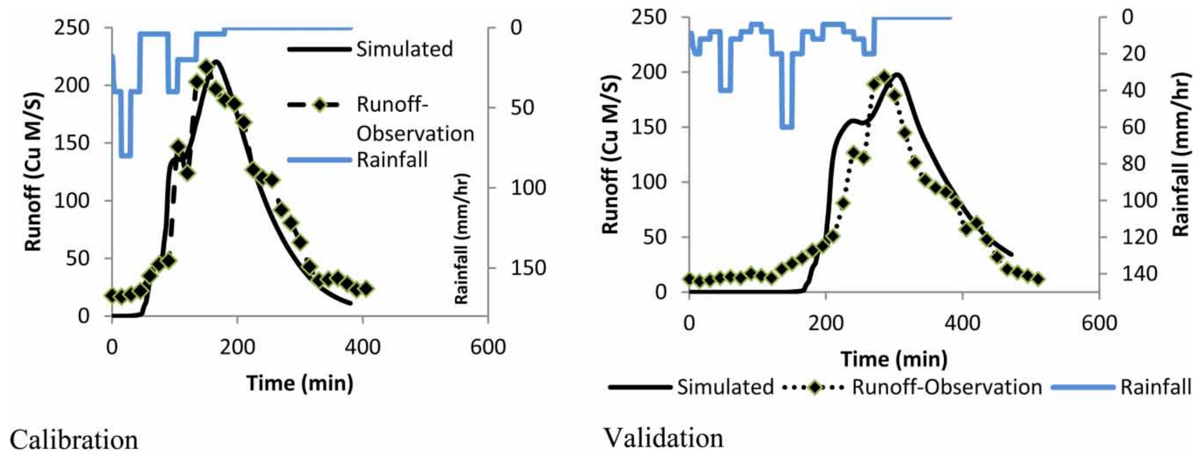

Figure 4 | Calibration and validation between K2-simulated and observed runoff.

Flood extent and hazard map

In Figure 5, the blue color represents the flooded area. The map is in TIN format, showing only elevations. These range from 5 to approximately 1,400 m. Flooding occurs mainly in lowland areas, which are shown clearly on the map. The map shows the extent of the flood at peak flow for a return period of 100 years with a 120-minute rainfall duration. The total area of inundation is approximately 20.52 km^2.

Flood depth

Nineteen scenarios were studied using different combinations of return period and duration. The model results show flood depths of up to 18 m (return period 100 years, duration 120 minutes). The greatest flood depth occurred upstream on the main channel, in a largely undeveloped area–perhaps because of the rapid discharge to the main channel there.

Downloaded from https://iwaponline.com/wpt/article-pdf/11/2/373/381751/wpt0110373.pdf
by guest

Water Practice & Technology Vol 11 No 2
doi: 10.2166/wpt.2016.044

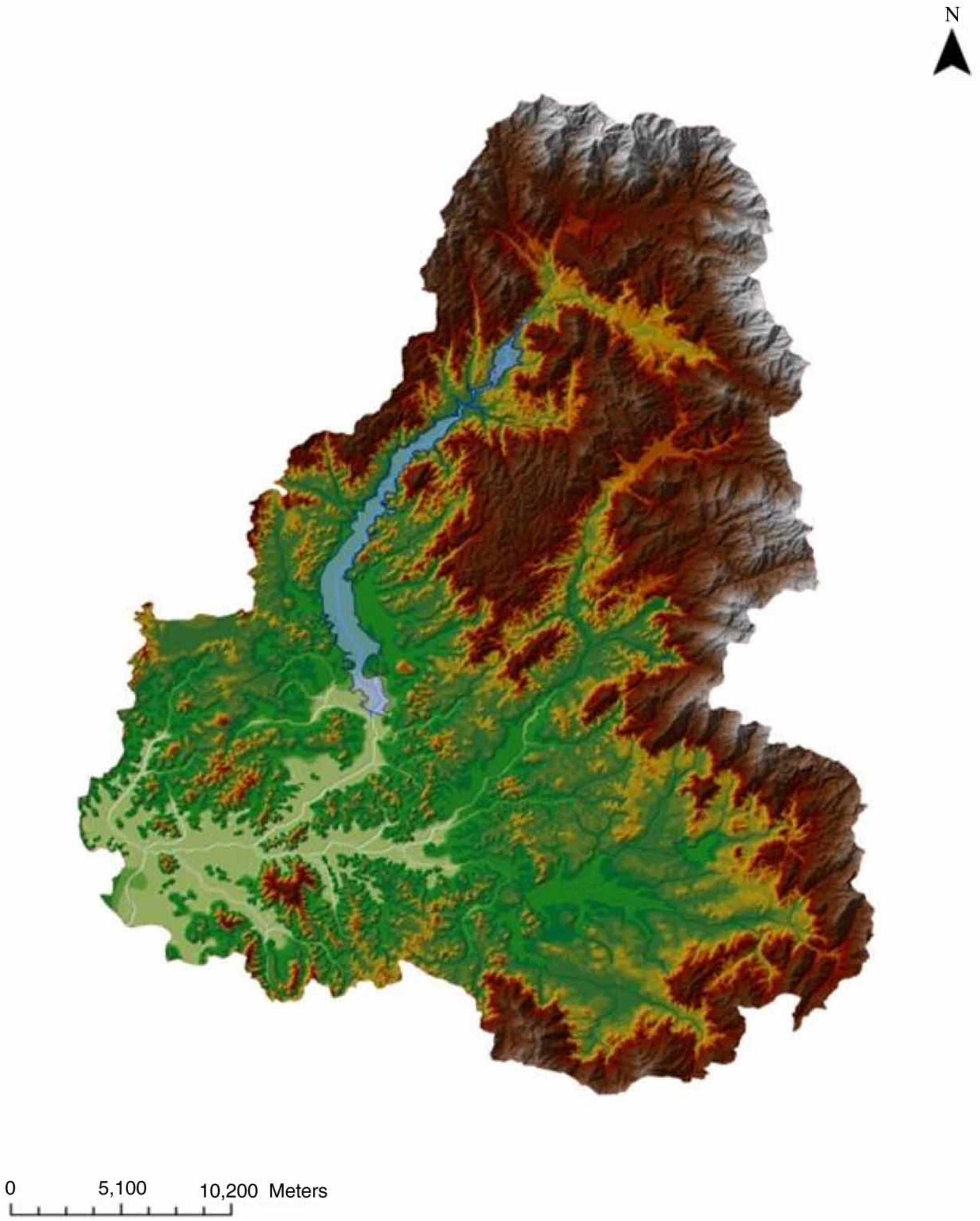

Figure 5 | Inundation Map for the Langat River, produced by modeling with K2 and HEC-GeoRAS.

Even downstream on the river, the water depth is still high, ranging from 2 to 10 m (Figure 6). There are many more people in these areas and, in future, when 100-year return period event occurs, large numbers will be affected, if no precautions are taken.

Figure 7 shows comparative curves for 5-, 25-, 50- and 100- year return period events, all with 120-minute duration.

Flow velocity

As the return period increases, the peak flow becomes greater because the hydraulic radius increases with flood depth, leading to an increase in velocity. The highest velocities reported from the model

Downloaded from https://iwaponline.com/wpt/article-pdf/11/2/373/381751/wpt0110373.pdf
by guest

Water Practice & Technology Vol 11 No 2
doi: 10.2166/wpt.2016.044

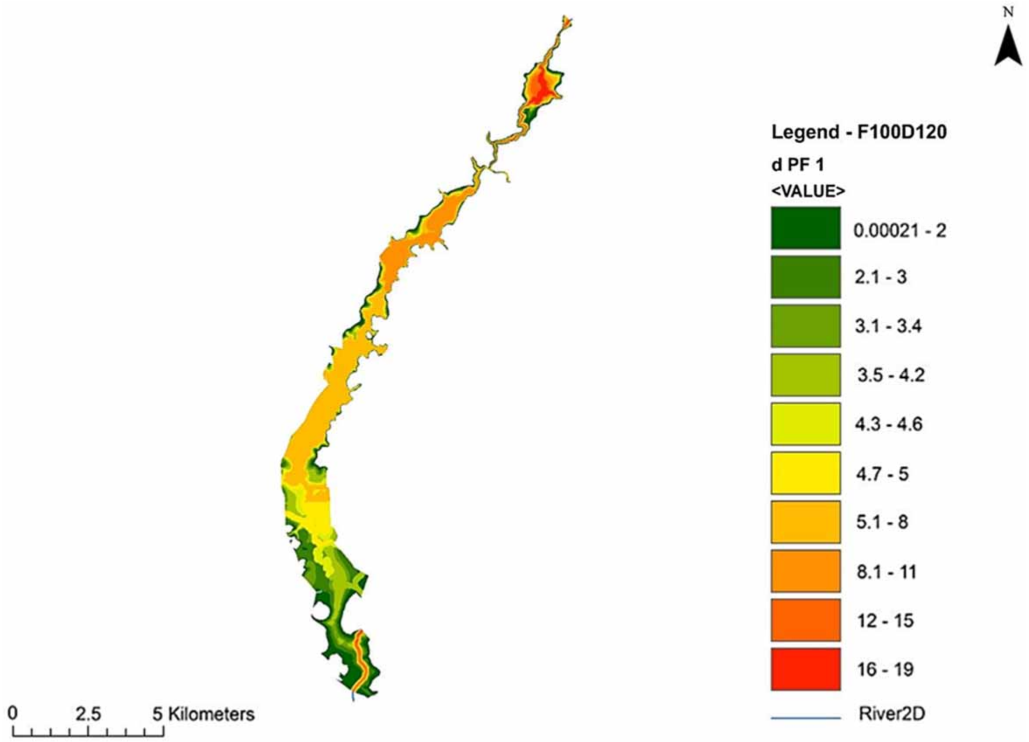

Figure 6 | Flood depths for 100-year return period and 120 minute duration.

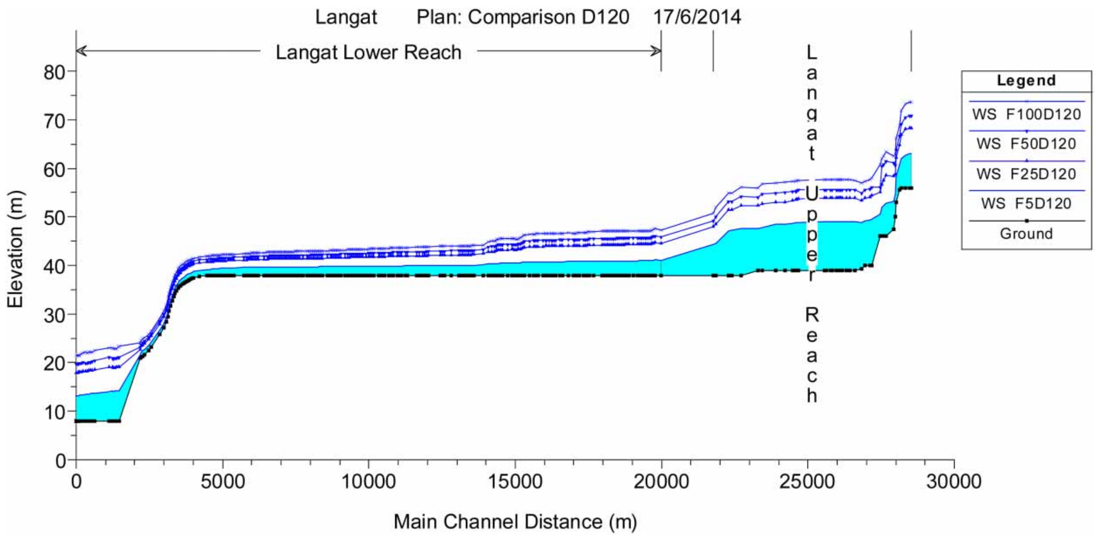

Figure 7 | Longitudinal section of the Langat River showing the water surface elevation for 120-minute storms with return periods of 5-, 25-, 50-, and 100- years (HEC-RAS model).

was 9.11 m/s, occurring mostly in the main channel upstream and the lowest reaches downstream. Again, they were related to the 120 minute, 100-year return period event (Figure 8).

For the 5-year return period events the maximum flow velocity is almost the same, at around 6 m/s, with storms of 60-, 90- and 120- minutes duration (Figure 9). Likewise, for the 25-year return period storms of the same durations, the maximum velocity is 8 m/s. While, for the 50-year return period storm of 120-minute duration 120, the maximum velocity is 9.11 m/s in the upstream section of the river. (For the 100-year return period, 30 and 90 storm events, the maximum velocity is approximately 9 m/s.)

Downloaded from https://iwaponline.com/wpt/article-pdf/11/2/373/381751/wpt0110373.pdf
by guest

Water Practice & Technology Vol 11 No 2
doi: 10.2166/wpt.2016.044

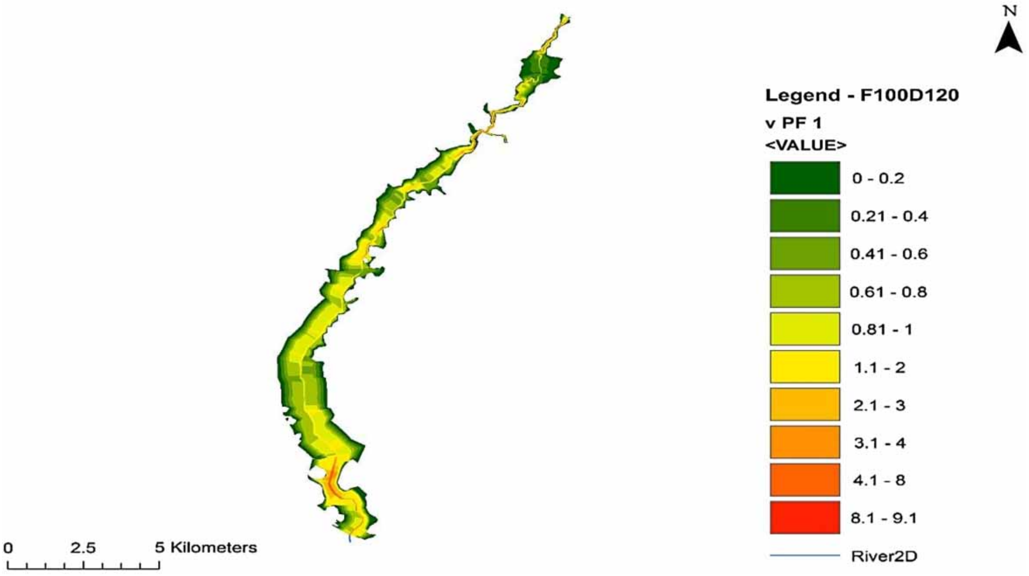

Figure 8 | Modeled flow velocities (HEC-RAS) for 120-minute duration, 100-year return period event.

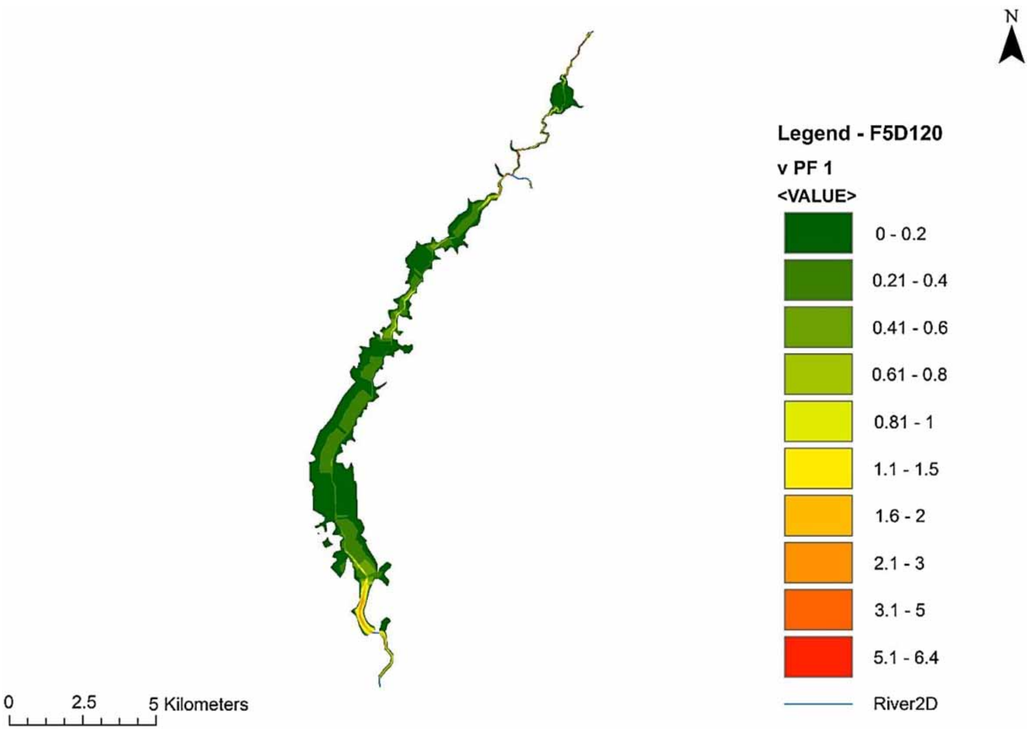

Figure 9 | Modeled flow velocities in the Langat River for a 5-year return period storm of 120 minutes duration.

CONCLUSIONS

Peak flows on the Langat River have been forecast with respect to rainfall events of different durations and return periods using the K2 model. The maximum peak flows related to different return period storms of different durations were also obtained.

Different water levels corresponding to different return period/duration storms were simulated using HEC-RAS. The maximum flood depth for the 100-year return period event of 120-minute duration is 18 m, while for the 15-minute 5-year return period event, it is 11 m.

Downloaded from https://iwaponline.com/wpt/article-pdf/11/2/373/381751/wpt0110373.pdf
by guest

doi: 10.2166/wpt.2016.044

Flow velocities corresponding to different storm return periods and durations were also simulated with HEC-RAS. For the 100-year return period storm of 120-minutes duration, the maximum velocity is 9.11 m/s, while for the 5-year return period 15-minute event, the maximum velocity is 2.5 m/s.

Using ArcGIS, it is possible to concentrate on the hydraulic model rather than preparing the data. Incorporating ArcGIS in the modeling can improve the accuracy of forecasting and save costs, subject to the quality of the TIN map.

Flood inundation prediction under different probabilistic scenarios can be used as a basis for floodplain risk management, as well as planning agricultural, industrial and urban expansion. It is important to locate new developments in areas of lower flood risk along the rivers, to minimize the potential social and economic impacts of flood hazard.

REFERENCES

Brilly, M., Rusjan, S. & Vidmar, A. 2006 Monitoring the impact of urbanisation on the Glinscica stream. *Physics and Chemistry of the Earth, Parts A/B/C* **31** (17), 1089–1096. Doi:10.1016/j.pce.2006.07.005.

Brunner, G. W. 2001 HEC-RAS River Analysis System. Army Corps of Engineering, p. 262.

Brunner, G. W. 2006 HEC-RAS, River Analysis System User's Manual, Version 4.0 Beta. U.S. Army Corps of Engineers, p. 420.

Goodarzi, E., Mirzaei, M. & Ziaei, M. 2012 Evaluation dam overtopping risk based on univariate and bivariate flood frequency analyses. *Canadian Journal of Civil Engineering* **39**, 374–387.

Goodrich, C. A., Wlotzka, F., Ross, D. K. & Bartoschewitz, R. 2006 NWA 1500: plagioclase-bearing monomict ureilite or ungrouped achondrite? *Meteorit. Planet. Sci.* **41**, 925–952.

Hicks, D. M. & Mason, P. D. 1998 *Roughness characteristics of New Zealand rivers*. National Institute for Water and Atmospheric Research–Water Resources Publications. LLC, Wellington, NZ, p. 329.

Howard, D. A., Luzzadder-Beach, S. & Beach, T. 2012 Field evidence and hydraulic modeling of a large Holocene jökulhlaup at Jökulsá á Fjöllum channel, Iceland. *Geomorphology* **147–148**, 73–85.

Merwade, V., Cook, A. & Coonrod, J. 2008 GIS Techniques for creating river terrain models for hydrodynamic modeling and flood inundation mapping. *Environmental Modelling & Software* **23** (10–11), 1300–1311. Doi:10.1016/j.envsoft.2008.03.005.

Miller, S., Semmens, D., Miller, R., Hernandez, M., Goodrich, D., Miller, W., Kepner, W. & Ebert, D. 2002

Mirzaei, M., Galavi, H., Faghih, M., Huang, Y. F., Lee, T. S. & El-Shafie, A. 2013 Model calibration and uncertainty analysis of runoff in the Zayanderood River basin using generalized likelihood uncertainty estimation (GLUE) method. *Journal of Water Supply: Research and Technology – AQUA* **62**(5) 309–320.

Mirzaei, M., Huang, Y., Lee, T. S., El-Shafie, A. & Ghazali, A. 2014 Quantifying uncertainties associated with rainfall depth duration frequency curves. *Natural Hazards-Springer* **71** (2), 1227–1239. DOI 10.1007/s11069-013-0819-3.

Moriasi, D. N., Arnold, J. G., van Liew, M. W., Bingner, R. L., Harmel, R. D. & Veith, T. L. 2007 Model evaluation guidelines for systematic quantification of accuracy in watershed simulations. *Trans. ASABE* **50** (3), 885–900.

Nash, J. E. & Sutcliffe, J. V. 1970 River flow forecasting through conceptual models: Part 1. A discussion of principles. *J. Hydrol.* **10** (3), 282–290.

Nedkov, S. & Burkhard, B. 2011 Flood regulating ecosystem services–mapping supply and demand, in the Etropole municipality. *Bulg. Ecol. Indic.* **21**, 67–79.

Nikolova, M., Nedkov, S., Nikolov, V., Zuzdrov, I., Genev, M., Kotsev, T., Vatseva, J. & Krumova, J. 2009 Implementation of the 'KINEROS' model for estimation of the flood prone territories in the Malki Iskar River Basin. *Information & Security: An International Journal* **24**, 76–88. Doi:10.11610/isij.2408.

Prata, D., Marins, M., Sobral, B., Conceição, A. & Vissirini, F. 2011 Flooding analysis, using HEC-RAS modeling for Taquaraçu river, in Ibiraçu city, Espírito Santo, Brazil. In: *12th International Conference on Urban Drainage*, Porto Alegre/Brazil, 11–16 September 2011. pp. 11–16.

Solaimani, K. 2009 Flood forecasting based on geographical information system. *African Journal of Agricultural Research* **4** (10), 950–956.

Woolhiser, D. A., Smith, R. E. & Goodrich, D. C. 1990 KINEROS, Kinematic Runoff and Erosion Model: Documentation and User Manual. USDA-ARS, No. 77.

Zakaria, S. 2008 *Case Study: Management Instruments for Langat River Basin,* pp. 1–48.

Downloaded from https://iwaponline.com/wpt/article-pdf/11/2/373/381751/wpt0110373.pdf
by guest